Research Paper

On the origin & thermal stability of Arrokoth's and Pluto's ices

C.M. Lisse [a,*], L.A. Young [b], D.P. Cruikshank [c], S.A. Sandford [c], B. Schmitt [d], S.A. Stern [b], H.A. Weaver [a], O. Umurhan [c], Y.J. Pendleton [e], J.T. Keane [f], G.R. Gladstone [g,s], J.M. Parker [b], R.P. Binzel [h], A.M. Earle [h], M. Horanyi [i], M.R. El-Maarry [j,y], A.F. Cheng [a], J.M. Moore [c], W.B. McKinnon [k], W.M. Grundy [l], J.J. Kavelaars [m], I.R. Linscott [n], W. Lyra [o], B.L. Lewis [p,q], D.T. Britt [r], J.R. Spencer [b], C.B. Olkin [b], R.L. McNutt [a], H.A. Elliott [g,s], N. Dello-Russo [a], J.K. Steckloff [t,u], M. Neveu [v,w], O. Mousis [x]

[a] Space Exploration Sector, Johns Hopkins University Applied Physics Laboratory, 11100 Johns Hopkins Rd, Laurel, MD 20723, USA
[b] Southwest Research Institute, Boulder, CO 80302, USA
[c] Astrophysics Branch, Space Sciences Division, NASA/Ames Research Center, Moffett Field, CA 94035, USA
[d] Université Grenoble Alpes, CNRS, CNES, Institut de Planétologie et Astrophysique de Grenoble, Grenoble, France
[e] Solar System Exploration Research Virtual Institute, NASA/Ames Research Center, Moffett Field, CA 94035, USA
[f] Astrophysics and Space Sciences Section, Jet Propulsion Laboratory/Caltech, Pasadena, CA 91109, USA
[g] Southwest Research Institute, San Antonio, TX 28510, USA
[h] Dept. of Earth, Atmospheric, and Planetary Sciences, Massachusetts Institute of Technology, Cambridge, MA 02139, USA
[i] Laboratory for Atmospheric & Space Physics, University of Colorado, Boulder, CO 80303, USA
[j] Birkbeck, University of London, WC12 7HX London, UK
[k] Department of Earth and Planetary Sciences and McDonnell Center for Space Sciences, One Brookings Drive, Washington University, St. Louis, MO 63130, USA
[l] Lowell Observatory, 1400 West Mars Hill Road, Flagstaff, AZ 86001, USA
[m] NRC Herzberg Inst of Astrophysics, 5071 W Saanich Road, Victoria, V9E 2E7 BC, Canada
[n] Hansen Experimental Physics Laboratory, Stanford University, Stanford, CA 94305-9515, USA
[o] Dept. of Astronomy, New Mexico State University, PO BOX 30001, MSC 4500, Las Cruces, NM 88003-8001, USA
[p] Department of Astronomy, Columbia University, 550 W. 120th St., New York, NY 10027, USA
[q] Division of Astronomy and Astrophysics, University of California, Los Angeles, 475 Portola Plaza, Los Angeles, CA 90025, USA
[r] Department of Physics, University of Central Florida, Orlando, FL 32816, USA
[s] Physics and Astronomy Department, University of Texas at San Antonio, San Antonio, TX 78249, USA
[t] Planetary Science Institute, Tucson, AZ 85719, USA
[u] Department of Aerospace Engineering and Engineering Mechanics, University of Texas at Austin, Austin, TX, 78712, USA
[v] Department of Astronomy, University of Maryland College Park, College Park, MD 20742, USA
[w] NASA/Goddard Space Flight Center, Planetary Environments Laboratory, Greenbelt, MD 20771, USA
[x] Aix-Marseille Université, CNRS, CNES, LAM, Marseille, France
[y] University College London (UCL), University of London, WC1E 6BT, London, United Kingdom

ARTICLE INFO

ABSTRACT

In this paper we discuss in a thermodynamic, geologically empirical way the long-term nature of the stable majority ices that could be present in Kuiper Belt object (KBO) 2014 MU$_{69}$ (also called Arrokoth; hereafter "MU$_{69}$") after its 4.6 Gyr residence in the Edgeworth-Kuiper belt (EKB) as a cold classical object. We compare the upper bounds for the gas production rate ($\sim 10^{24}$ molecules/s) measured by the New Horizons (NH) spacecraft flyby on 01 Jan 2019 to estimates for the outgassing flux rates from a suite of common cometary and KBO ices at the average ~ 40 K sunlit surface temperature of MU$_{69}$, but do not find the upper limit very constraining except for the most volatile of species (e.g. CO, N$_2$, CH$_4$). More constraining is the stability versus sublimation into vacuum requirement over Myr to Gyr, and from this we find only 3 common ices that are truly refractory: HCN, CH$_3$OH, and H$_2$O (in order of increasing stability), while NH$_3$ and H$_2$CO ices are marginally stable and may be removed by any positive temperature excursions in the EKB, as produced every 10^8–10^9 years by nearby supernovae and passing O/B stars. To date the NH team has reported the presence of abundant CH$_3$OH and H$_2$O on MU$_{69}$'s surface (Stern et al., 2019; Grundy et al.,

---

* Corresponding author at: Planetary Exploration Group, Space Exploration Sector, Johns Hopkins University, Applied Physics Laboratory, SES/SRE, Bldg 200, E206, 11100 Johns Hopkins Rd, Laurel, MD 20723, USA.

E-mail address: carey.lisse@jhuapl.edu (C.M. Lisse).

2020). NH$_3$ has been searched for, but not found. We predict that future absorption feature detections, if any are ever derived from higher signal-to-noise ratio spectra, will be due to an HCN or poly-H$_2$CO based species. Consideration of the conditions present in the EKB region during the formation era of MU$_{69}$ lead us to state that it is highly likely that it "formed in the dark", in an optically thick mid-plane, unable to see the nascent, variable, highly luminous Young Stellar Object (YSO)/TTauri Sun, and that KBOs contain HCN and CH$_3$OH ice phases in addition to the H$_2$O ice phases found in their short period (SP) comet descendants. Finally, when we apply our ice thermal stability analysis to bodies/populations related to MU$_{69}$, we find that methanol ice is likely ubiquitous in the outer solar system; that if Pluto isn't a fully differentiated body, then it must have gained its hypervolatile ices from proto-planetary disk (PPD) sources in the first few Myr of the solar system's existence; and that hypervolatile rich, highly primordial comet C/2016 R2 was placed onto an Oort Cloud orbit on a similar few Myr timescale.

1. Introduction

On 01 Jan 2019, the New Horizons spacecraft visited for the first time ever a small, pristine cold classical Kuiper Belt object (KBO), Arrokoth (2014 MU$_{69}$; hereafter MU$_{69}$). Resolved multiband photometric imaging and near-infrared (NIR) spectroscopy were obtained of MU$_{69}$'s surface, producing a picture of a dark, highly reddened object containing solid water ice, methanol, and tholins (Stern et al., 2019) and no detectable gas in any surrounding coma.

Because its orbit is nearly circular and uncoupled to the solar system's planets, MU$_{69}$ is thought to have formed in place 4.6 Gyrs ago at ~45 AU, and could contain one of the most primitive collections of early solar system material studied to date. Naively, one might think that its current low ambient dayside average temperature of ~42 K should have kept most icy species in "deep freeze", leaving them unreacted and unchanged since their formation. The ice species of interest include those detected on planetary satellites, Centaurs, Pluto, and KBOs in the outer Solar System like H$_2$O, CH$_4$, N$_2$, CO, CO$_2$, CH$_3$OH (methanol), HCN
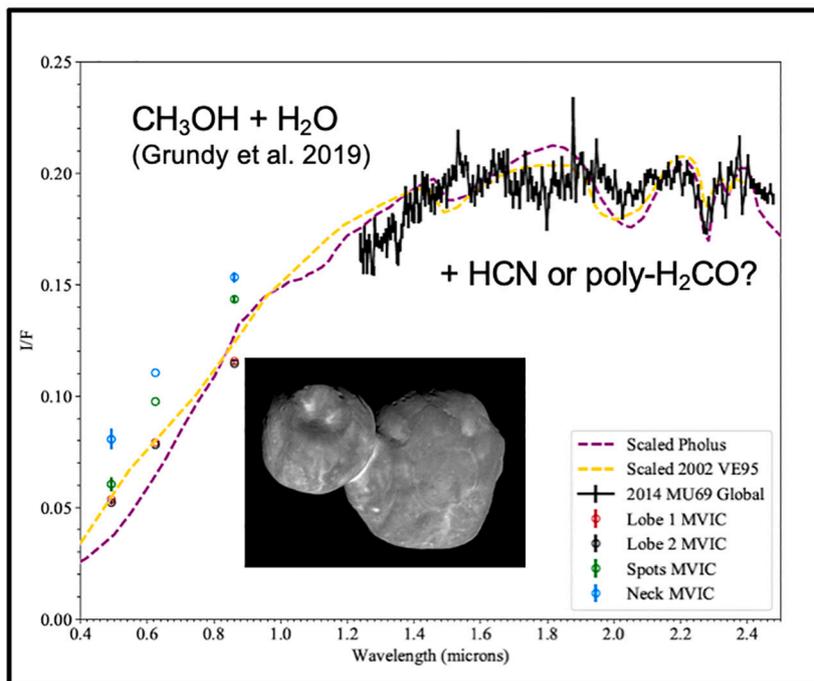
Fig. 1. Ices found on Arrokoth (top) and Pluto (bottom) by using New Horizons' Ralph/LEISA instrument suite to create spectrophotometric maps of the bodies. MU$_{69}$'s surface is dominated by strong, nearly uniform signatures of CH$_3$OH and a reddish-orange tholin, and weak signatures of H$_2$O. In stark contrast, Pluto's surface is dominated by CH$_4$, N$_2$, CO, and reddish "Pluto tholin".

(hydrogen cyanide), $NH_3 \bullet nH_2O$ (ammonia hydrate), and C_2H_6 (ethane); and those detected in cometary comae as the products of nuclear mass loss, such as C_2H_2, C_3H_8, SO_2, and O_2 (Bieler et al., 2015, Mall et al., 2016).

However, while CH_3OH was found from two well-defined absorption bands at 2.27 and 2.34 μm by the New Horizons Linear Etalon Imaging Spectral Array LEISA (LEISA) 1.25–2.5 μm mapping spectrometer ($\lambda / \Delta\lambda = 240$ and MU69 spatial resolution ~1.8 km px^{-1} on a 33 × 17 km object; Reuter et al., 2008, Stern et al., 2019, Spencer et al. 2019; Fig. 1), H_2O signatures were only weakly present if at all (as seen by a broad H_2O absorption band centered at 2.0 μm; Lisse et al., 2017, Grundy et al., 2020). As for CH_4, none of the multiple prominent absorption bands in the LEISA spectral range were seen. Nor were the extremely "hyper-volatile" species CO and N_2 detected. Among the weakly absorbing species, the important candidate molecule HCN has three small absorption bands in the LEISA range ($2\upsilon_3$ at 2.432 μm, $(\upsilon_1 + \upsilon_3)$ at 1.866 μm, and $2\upsilon_1$ at 1.535 μm; Quirico et al., 1999), that could not be discerned within the noise pattern of the spectra obtained. Similarly, CO_2 was not detected; its principal signature in the LEISA spectral range consists of three narrow and relatively weak bands near 2.0 μm which, if present, could not be discerned at the noise level achieved in the data. ((The returned spectra, while revolutionary for such a small KBO, were also at the same time limited by the finite pixel scale and rapid scan pattern of the fast New Horizons flyby.)

In this paper, we seek to provide a thermal stability interpretation for the observed composition of MU69's surface. To this end, we utilize thermodynamical studies of laboratory analogue ice vapor pressures and find that almost all of the primitive ices known to be in outer solar system icy bodies should have been removed long ago from a nigh-gravitationless MU69. Our analysis suggests that only the high boiling temperature (hereafter "refractory"), hydrogen-bonded ice species H_2O, poly-H_2CO, CH_3OH, and HCN, as well as minority impurities in refractory-ice phases, should be present if accreted by MU69 4.6 Gyr ago.

Our analysis also reproduces the observed mix of solid, stable ices on Pluto's surface and the $N_2/CO/CH_4$ found in its atmosphere (Grundy et al., 2016; Fig. 1).

We interpret the surface composition to also reflect the bulk composition of MU69 and other distant small bodies with a similar dynamical history. Although in principle the New Horizons LEISA spectra and MVIC 4-color photometric maps (Stern et al., 2019; Grundy et al., 2020) characterize only the first few optically active microns of MU69 surface, they show a remarkably homogenous surface throughout terrain that varies kilometers in relief across hills, valleys, rills, and crater floors on the surface of a markedly flattened object only a few kilometers thick. Further, when we look by extension to other similar distant EKB bodies in the same thermal zone, like Plutino (55638) 2002 VE95 and distant Centaur 5145 Pholus, we see similar compositional spectra (Fig. 1). Yet when we follow these objects in, we see them become active and lose their abundant methanol, and convert to the water ice dominated inner centaurs and short period comets. None of these objects show any evidence for abundant (vs water) hypervolatiles such as the CO, N_2, and CH_4 seen on Pluto and the larger KBOs. There has, however been one recent small icy body counterexample that does appear to be just as expected for a small, primordial hypervolatile-rich object - Comet C/2016 R2, known for its large outgassing of CO and N_2 but not H_2O. As we discuss below, this makes sense if R2 has retained its hypervolatile ices to the present day, and is only now subliming some of them while keeping the rest of its volatile ices ultra-cold, stable, and rock hard via sublimative cooling.

Section 1 of this paper is intended to present the known observational results for ices in MU69 from the New Horizons flyby. Each of these results alone is moderately useful, but the combination of surface spectral mapping, UV coma non-detection, and rotationally resolved whole body imaging provide powerful constraints on the nature of the body. In Section 2 we present the details of our thermodynamic calculations and the resulting saturation vapor pressure versus temperature
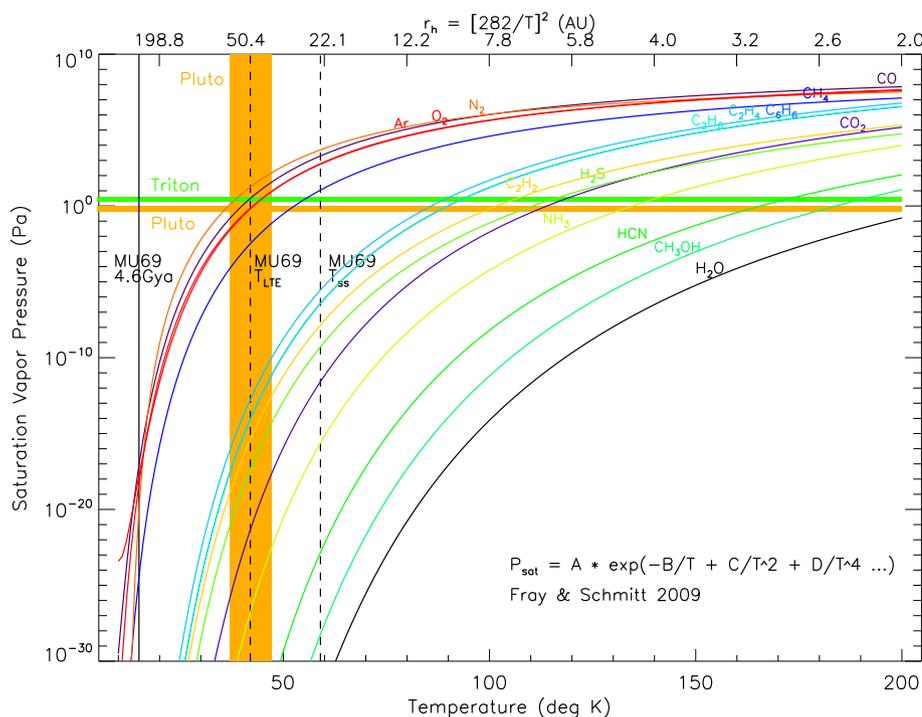
Fig. 2. Saturation pressure P_{sat} as a function of temperature for 12 common species found in small solar system body ices. The range of saturation pressure curve behavior ranges from hypervolatile (N_2, CO, O_2, Ar, CH_4) at upper left to highly refractory (HCN, CH_3OH, H_2O) at lower right. In the mid-range are a host of medium-volatile hydrocarbon species. Also shown is the range of temperatures (37 to 47 °K) and pressures (~10 μbar) on Pluto's surface determined by New Horizons (intersection of horizontal and vertical gold bars). By comparing to our model P_{sat} curves, it can be seen that only the hypervolatile ices will be in the gas phase on Pluto, and that in some regions they will be stable solids.

MU₆₉ Today
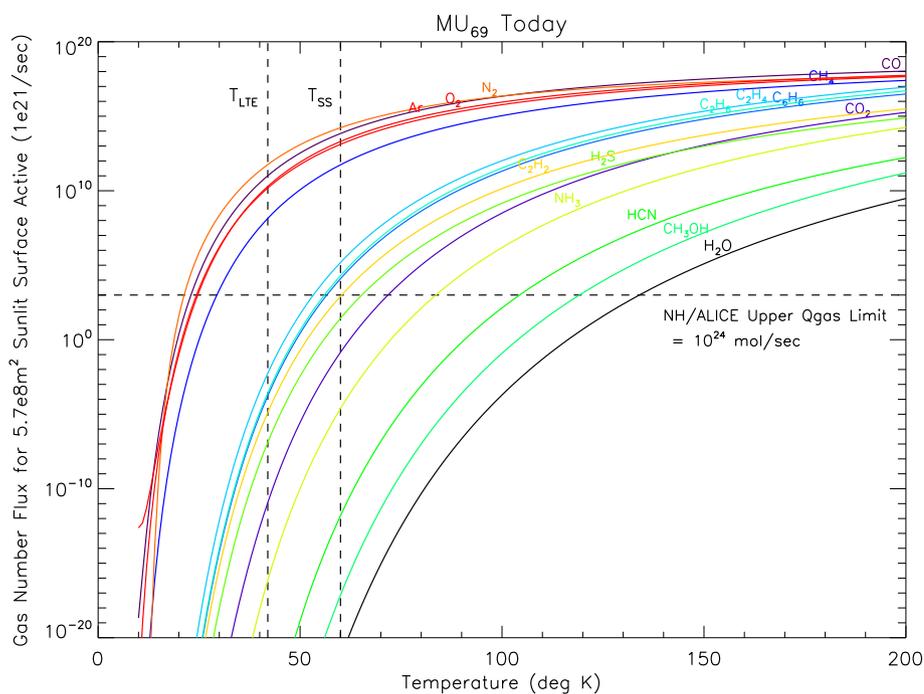
Fig. 3. Plot of total Q_{gas}, the total production rate of gas molecules for a given ice species from MU₆₉, vs ambient temperature, assuming the ice species is uniformly distributed across MU₆₉'s sunlit side. The non-detection for gas production produced using the NH/ALICE spectrometer's measurements (of H_2) is shown by the dashed line. If the surface of MU₆₉ contained appreciable N_2, CO, O_2, Ar, or CH_4 icy material at ~42 K in thermal contact with the surface, we would have detected its gas molecule emission rate above the limiting sensitivity of the ALICE measurements.

(P$_{sat}$ vs T) curves.[1] In this Section we also calculate the upper limits for the surface area of any currently exposed sublimating ices presented by the non-detection of a gas coma around MU₆₉ by New Horizons.

Using these laboratory measured heat of sublimation values, in Section 3 we then show that if low boiling point temperature molecular ice species like N_2, CO, or CH_4 (hereafter "hypervolatile ices") were *ever* incorporated into MU69 as majority ice phases, then they are not only not there today, but they shouldn't have been there after the first few Myr of its existence. By contrast, high boiling point temperature hydrogen bonded ice species like H_2O, CH_3OH, or HCN (hereafter "refractory ices") incorporated as majority phases into MU69 4.56 Gyrs ago should still be there today, stable as rock.

The final sections of the paper are interpretive of the facts established in the first two sections. In Sections 4 we show analytically how thermally driven icy body evolution can explain the NH findings for MU69. In Section 5 we extend our analysis via logical

arguments to predictions bearing further verification concerning the compositional connections between KBOs, Centaurs, and Comets, the expected abundant refractory ices composing the Pluto system's bodies, and the curious hypervolatile rich counter-case of Comet 2016 R2.[2]

2. Thermodynamical background

Investigations on the subject of the stability of EKB ices have been conducted intermittently in the literature over the last few decades. We review the major efforts here in order to provide the reader with a useful summary of previous thought and likely avenues for future research and progress. (This work, for example, was inspired by our 2019 understanding that updated laboratory cryogenic heat of sublimation measurements produced by KBO astronomers have not yet been applied to the small icy body sublimation models produced by cometary astronomers or the hot core ice models of astrophysicists.)

Starting in the late 1980s, astronomical infrared spectral studies investigating the composition of icy molecular cloud cores, the precursors to solar systems and their icy planetesimals, detected absorption features indicative of ices containing H_2O, CO, CO_2, CH_4, H_2CO, NH_3,

---

[1] Section 2 and the SOM are important for explicitly writing down for both the KBO and the Comet communities' use the temperature dependence of ice vapor pressure for the dominant ice species expected in outer solar system icy bodies. In doing this, we employ the measured heats of vaporization for the pure ice species which are readily obtainable from terrestrial laboratory measurements. Real KBO ices are likely to be some sort of mixture of pure and compounded (or alloyed, or mixed; in this paper we use the terms interchangeably) ices, due to the chaotic messiness of planetesimal formation in the early solar system, with a PPD likely dominated by number by simple H_2O, CO, and N_2 molecules plus heavier species created via heterogenous catalysis on grain surfaces (e.g. Nuth et al., 2008). Add to this the vagaries of the temperature and density structure of the convecting PPD, the effects of protoplanet disk stirring, and the behavior of stochastic solar FU Ori/EX Lupi accretion events and XUV stellar outbursts over time, and it is quite difficult to state with any certainty the exact nature (pure, mixed, alloyed, or crystalline) of the ices first incorporated into proto-KBO bodies. Until we have a cryogenic core sample of these ices in a terrestrial laboratory for measurement, we will not know which of a nearly infinite possible mixed phases we should measure; fortunately the properties of many possible combinations of mixed ices have been studied by the Ames group in the 90's [c.f. Sandford et al. 1988, 1990, 1993], and they grossly tend to follow the dominant ice species' behavior, which we study here.

[2] Caveat: By no means is this treatment meant to replace detailed time-dependent modeling of a 3-dimensional representation of KBO, which is why we do not delve deeply in this paper into the details of the first few Myrs of Arrokoth's life - which must have been very interesting and variable, although transient. The purpose of this paper is to set up the problem of the possible icy constituents of KBO MU₆₉ and Pluto as seen today after 4.56 Gyr of thermal evolution. I.e., to state what we know for sure from simple thermodynamic and geophysical considerations, while avoiding the uncertainties in important parameters like the runs of interior density, thermal heat capacity, and thermal conductivity through the body that produce a variety of outcomes in more detailed models. We hope that this work and its given material abundance restrictions inspires future detailed modeling work that will fill in more of the picture, especially the short-term time dependent behavior of KBO interiors over the first few Myr, by studying the extent of modeling phase space in the manner of Prialnik et al. (2004), Merk and Prialnik (2006), and Rosenberg and Prialnik (2009).

and CH_3OH (Tielens et al. 1989, Allamandola et al., 1992, Lacy et al., 1998). The spectral and physical properties of these ices, including their sublimation and condensation behaviors, were studied in the laboratory (e.g., Sandford and Allamandola, 1988, 1990, 1993a, 1993b; Schutte et al., 1993a, 1993b) to investigate the possible makeup of these clouds, and the plausibility that the laboratory ice analogues could be present in the molecular cloud at the ambient temperatures estimated from their spectroscopy. This work produced surface binding energy estimates for the various ices, useful for producing stability ages for their solid, icy phases assuming the relative "sticking probabilities" of molecules as a function of temperature.

For a gaseous species in chemical equilibrium with its solid phase the dependence of its saturation vapor pressure is given by the Clausius-Clapeyron thermodynamic equation:

$$1/P \, dP_{sat}/dT = \mu H_{subl}/R_g T^2 \tag{1}$$

with solution $P_{sat} = C*exp.^{(-\mu Hsubl/RgT)}$. Here, P_{sat} is the saturation vapor pressure above a patch of ice, T is the ice temperature, μ is the mass of 1 mol of gas, H_{subl} denotes the enthalpy (i.e., latent heat) of sublimation per kg, and $R_g = N_{Avogadro}*k_{Boltzmann}$ is the ideal gas constant. Assuming that H_{subl} is independent of temperature, Prialnik et al. (2004), following up on earlier laboratory work in forming and evolving analogue icy cometary materials (Yamamoto et al., 1983; Bar-Nun et al., 1985, 1987; Prialnik et al., 1987, 1990; Schmitt 1989, 1992), used this relation together with empirically tabulated $P_{sat}(T) = A * exp.^{(-B/T)}$ fits known since the 1920s to obtain and tabulate its exponential coefficient in terms of the latent heat (SOM Table 1). The form of these P_{sat} curves is such that they all have a universally similar structure with rapidly rising pressures and "knees" controlled by the value of $(H_{subl}/k_{Boltzmann})$, i.e. the heat of sublimation expressed in Kelvin. Fig. 2 shows examples of these curves, where it can be seen that ices which sublime easily (like hypervolatile molecular solids N_2, CO, and CH_4 with only van der Waals molecule-molecule interactions) have small values of $H_{subl}/k_{Boltzmann}$, on the order of 10^2 K, while refractory ices (like the hydrogen-bonded species H_2O, H_2CO, CH_3OH, HCN, and NH_3 with relatively strong inter-molecular bonds) have $H_{subl}/k_{Boltzmann}$ values in the many-thousands (e.g. Sandford & Allamandola 1993a, 1993b).

The flux rate at which an icy cometary material loses molecules into a surrounding medium follows from gas kinetic theory (Prialnik et al., 2004) as.

$$Z \, (molecules/m^2/s) = \rho_{gas}*v_{gas} = (P_{sat} - P_{ambient})/kT*v_{thermal,z+} = (P_{sat} - P_{ambient})/(2\pi kTm)^{0.5} \tag{2}$$

where Z is the mean loss rate per unit normal surface area, the ideal gas law has been used to express the gas number density $\rho_{gas} = (N/V) = P/kT$, $v_{thermal,z+} = (kT/2\pi m)^{0.5}$ is the mean Maxwell-Boltzmann velocity at temperature T for gas molecules leaving perpendicular to the ice surface, m is the molecular gas mass, and k is Boltzmann's constant, respectively.

Once the proper local equilibrium temperature T is calculated (see Section 4.1), two important special cases of Eq. 2 occur: (1) When $P_{sat} < P_{ambient}$, as for a body with a stable atmosphere, no net molecules are actively emitted into the medium and the ice is thermally stable and remains condensed. This is the case studied in the seminal paper of Schaller and Brown (2007) predicting which of the largest KBOs could retain atmospheres and thus finite surface pressures, and which ices would be stable given the KBO's ambient temperature and pressure (Schaller and Brown, 2007, Brown et al. 2011). We can use this approach to predict the ices which should occur on Pluto's surface and in its atmosphere given the ~10 μbar of ambient surface pressure (as measured by New Horizons, Stern et al., 2015, Gladstone et al. 2017).

(2) When $P_{ambient} \approx 0$, in which case the ice is exposed to vacuum, and the derived sublimative flux rates can be compared to the ~10^{15}/

cm^2 molar surface densities of ices[3] to determine how long it takes for a patch of exposed ice to fully sublimate away. This case is analogous to the residence lifetime arguments of Langmuir (1916), Frenkel (1924), and Sandford et al., 1993, and can be used to predict the lifetime (versus thermal sublimation) of exposed ices on comet surfaces and in interstellar and interplanetary dust grains. These lifetimes are upper limits, as other removal processes, such as photon irradiation, stellar wind particle sputtering, and micrometeorite impact gardening can also remove mass from exposed ice.

To confirm which regime applies to MU_{69} and Pluto, we use the Catling and Zahnle (2009, 2017) airless body condition. A body can retain a stable atmosphere when

$$V_{thermal} = 0.8 \, km/s *(T/300K)^{0.5} << V_{escape} = (2GM_{KBO}/R_{KBO})^{0.5}$$
$$= (8\pi Gr\rho R_{KBO}^2/3)^{0.5} \approx 11 \, km/s *(R_{KBO}/6400km)^{2/3}*(\rho/5.2gcm^{-3})^{0.5} \tag{3}$$

while the $P_{ambient} \approx 0$ condition is pertinent when the opposite is true for a body, $V_{thermal} >> V_{escape}$. Evaluating, we have for Pluto that $V_{thermal} \sim 250–320 \, m/s < V_{escape} \sim 1200 \, m/s$, while for MU_{69}, $V_{thermal} \sim 290 \, m/s >> V_{escape} \sim 4 \, m/s$.

Fray and Schmitt (2009) revisited the problem of the temperature dependence of P_{sat}, going beyond the simple assumption of $H_{subl} = Constant$ and allowing for temperature variation of the heat of sublimation. After conducting an exhaustive literature search for relevant ice data, they reported results for more than 20 species in polynomial form, as $P_{sat} = A_0 + A_1/T + A_2*T^2 + A_3/T^3, + A_4/T^4 + A_5/T^5$ (reproduced here in SOM Table 2) greatly refining the accuracy of the P_{sat} curves, especially at low values of (R_gT/H_{subl}) where P_{sat} changes most rapidly. Since we are most interested in the behavior of ices in small outer solar system bodies at low temperatures (T = 10 to 90 K), we have adopted the more refined constants published by Fray and Schmitt (2009) (SOM Table 2) in calculating the values of P_{sat} for this work.

3. Results

Fig. 2 shows the resulting P_{sat} saturation pressure curves we have calculated from the Fray & Schmitt data. Some immediate findings can be made from them:

(1) As a check of our calculations, the P_{sat} values derived from Prialnik et al., 2004's $H_{subl} = constant$ approximation and the Fray and Schmitt, 2009 polynomial fits were compared, and found to match well at high temperatures $T > (H_{subl}/k)$ where the older values of H_{subl} were determined and the temperature dependence of H_{subl} is small.

(2) There are hypervolatile (N_2, CO, CH_4), mid-volatile (C_2H_2, C_2H_4, C_2H_6, C_6H_6, H_2S, CO_2, NH_3), and 'refractory' (HCN, CH_3OH, H_2O) ices in the list, with a broad range of outgassing rates at any given temperature.

(3) All but the most hypervolatile (N_2, CO, O_2, Ar, CH_4) species should be stable as rock-solid ices on the surface of Pluto today, with its ambient pressure of ~10 μbar = 0.1 Pa. The hypervolatile solid ice species should be in metastable equilibrium with the atmosphere, depending on the local surface temperature (ranging from 37 K in Sputnik Planitia to 45 K in Cthulhu Macula; Earle et al., 2017) and pressure (ranging from 11 μbar in lowland Sputnik Planitia to ~8 μbar in the mountain

---

[3] Molar surface density ~ $(\rho/MW * N_{Avogadro})^{0.67}$; for water ($H_2O$) with bulk density $\rho = 1 \, g/cm^3$ and MW = 18 g/mol, this is $1.0 \times 10^{15}/cm^2$ with 3.2×10^7 molecules/cm, or 3.1×10^{-8} cm/molecule= 3.1 Å/mol spacing. For methanol (CH_3OH) with bulk density $\rho = 0.8 \, g/cm^3$ and MW = 32 g/mole, its molar surface density is $(0.8/32 * 6 \times 10^{23})^{0.67} = 6.1 \times 10^{14}/cm^2$, and the intramolecular spacing is 10^8Å/cm/$(6.1 \times 10^{14}/cm^2)^{0.5} = 4.0$ Å/molecule. For HCN with bulk density $\rho = 0.7 \, g/cm^3$ and MW = 27 g/mole, its molar surface density is $(0.7/27 * 6 \times 10^{23})^{0.67} = 6.2 \times 10^{14}/cm^2$, and the intramolecular spacing is 10^8Å/cm/$(6.2 \times 10^{14}/cm^2)^{0.5} = 4.0$ Å/molecule.

highlands; Schmitt et al., 2017, Moore et al., 2018a, Moore et al., 2018b, Young et al., 2018, Betrand et al., 2019). This is consistent with New Horizons' determination of the (N_2, CO, CH_4) surface patterning and atmospheric makeup of Pluto (Stern et al., 2015; Gladstone et al., 2016; Young et al., 2018).

(4) For similar reasons, MU_{69}, with its $P \approx 0$ surface pressure, should be unable to retain the hypervolatile (N_2, CO, O_2, Ar, CH_4) species in the form of pure ices. At the local thermodynamic equilibrium temperature of ~42 K in its stable cold classical orbit, for an object with emissivity = 0.90 (Stern et al., 2019, Buratti et al. 2019, Verbiscer et al. 2019), these hypervolatile ices have high vapor pressures (as demonstrated by their presence in Pluto's atmosphere, above Pluto's even colder surface; Fig. 2). *In fact, these species should never have been condensed out of the gas phase in any appreciable amounts in the vacuum of space at current MU_{69} temperatures. For these gases to condense originally as dominant ice phases, MU_{69} would have had to have formed in a much colder locale*, as could be created by a proto-Edgeworth-Kuiper Belt heavily shrouded from the proto-Sun by an optically thick proto-planetary disk mid-plane. In this case, the lowest local temperatures would have been that of molecular clouds in the galactic interstellar medium (ISM) radiation field, or about 15 K. (Observations of currently extant exo-PPDs (e.g., Anderl et al., 2016, Öberg et al., 2017, Loomis et al., 2020) and models of the solar nebula and PPDs around Sun-like stars (e.g., Lesniak and Desch, 2011; Krijt et al., 2018, 2020; Mousis et al., 2019) have mid-plane temperatures at 45 AU from the Sun at T ~ 15 to 25 K within the first few Myr of the solar system's existence.) From Fig. 2, temperatures at this level can allow appreciable hypervolatile ice accumulation, and the detection of hypervolatile ices in interstellar dense clouds attests to this occurrence (Tielens et al. 1989, Allamandola et al., 1992, Lacy et al., 1998). But it is also during the first few Myr of a KBO's existence when short-lived radioactive nuclides like Al^{26} can cause substantial warming in the heart of a KBO (Choi et al. 2001, Prialnik, 2002, Prialnik et al., 2004), making the condensation of hypervolatiles problematic.

In the next section, we show that if bulk majority phase hypervolatile ices were initially incorporated into MU_{69}, then subsequent short-lived radioactive driven evolution would relegate them to near-surface regions, and that these regions will then become depleted within ~1 Myr of the present-day surface temperatures being established. We go on to state that the hypervolatile ice species CO and CH_4 we see outgassing from icy bodies today must have been stabilized over time by residing as a minority component in a non-pure ice whose thermal stability was controlled by a more refractory ice like CH_3OH or H_2O.

Observational support for the lack of hypervolatile ices (except as minority impurities in dominantly refractory ice phases) in MU_{69} is shown in Fig. 3. Here we have compared the 3-sigma upper limit on the gas production rate, Q_{gas}, supporting the gravitationally unbound atmosphere, or coma, surrounding MU_{69} as determined by NH/ALICE UV spectrometer solar Lyman-alpha airglow measurements during the 01 Jan 2019 flyby to our calculated net outgassing rate for ices mixed uniformly on the surface of a $T_{LTE} = 42$ K object of MU_{69}'s measured surface area. The published upper limit for Q_{gas} is ~10^{24} molecules/s (Stern et al., 2019), a relatively high rate of gas release at 45 au when compared to other actively subliming solar system bodies like comets at ~1 au (Lisse, 2002, Bockelee-Morvan et al. 2004). However, this value is sensitive enough to rule out uniform layers of hypervolatile CH_4 ice, and, by extension, (N_2, CO, O_2, and Ar), on direct measurement grounds, as these species would produce gas flux rates far above the upper limit rate (dashed line) in Fig. 3.

Further, if we note that MU69 had a special orientation geometry during the NH flyby such that one-half of its highly flattened surface was pointed nearly sunward while the other half was in near-total shadow, so that the sunlit side temperature was closer to $T_{ss} = 59$ K, then we see that the presence of even moderately volatile organic ice species like C_2H_2, C_2H_4, C_2H_6, and C_6H_6 is ruled out.

4. Discussion & analysis

More stringent constraints can be placed on ice stability if we consider not only their current sublimation loss rate, but their loss rate over the age of the Solar System and the age of MU_{69}. Using the outflux rates of Fig. 3, as a most-conservative case we can assume their stability over time in the EKB during their Gyrs-long post-aggregation phase, and see how long it takes a molar surface density's worth[1] (~10^{15}/cm^2 = 10^{19}/m^2) of material to be removed via thermal sublimation.

4.1. Negligible sublimative cooling after ~ 1 Myr

We can safely make an approximate calculation using simple thermodynamic and energy balance arguments on Gyr timescales for the following reason. The energy balance equation (neglecting any endogenic heat flux) for heating of a unit slab of KBO material (1 m wide by 1 m long by dz. thick) of Bond albedo A and effective thermal emissivity ε oriented at angle ξ at r_h distance from a 1 L_{sun} luminosity star is:

$$(1 - A)L_{sun}\cos\xi/4\pi r_h^2 = \varepsilon\sigma T^4 + \Sigma_i Z_i \Delta H_{subl,i} * \left(10^{-3} \text{ M.W.(g)}/N_{Avogadro}\right)_i \tag{4}$$

where the first term is any input insolation, the second is the re-emitted thermal radiation from the object, and the third is the cooling derived from sublimation of the object's volatile species. We look at the relative magnitudes of these terms by calculating the maximal possible rate of sublimative cooling vs. temperature possible for an icy species, using the gas production rate (Q_{gas}, in molecules/m^2/s) curves of Fig. 3 multiplied by the heat of sublimation ($H_{subl,i}$, in J/molecule sublimed) for a species. Fig. 4 shows the result, from which it can be seen that sublimative cooling is a negligible term for an object like MU_{69} in the Edgeworth-Kuiper Belt compared to the ~0.7 W/m^2 received from the Sun, except in the case of the hypervolatile species (CO, N_2, CH_4, Ar, and O_2). This result is also consistent with other ice sublimation modeling work, like that of Steckloff et al. (2015, 2020).

We have shown in Section 3 that there are no dominantly hypervolatile ice phases in abundance today on the surface of MU_{69}, and argued that it is unlikely that any majority hypervolatile ices ever did condense into the KBO unless it formed in a cold, optically thick mid-plane region of the PPD. In this eventuality, the effects of sublimative cooling due to hypervolatile evaporation would be short-lived. E.g., if we were to construct MU_{69} entirely out of albedo = 0.16 N_2 or CO ice with H_{subl} ~ 10^{-20} J/molecule (Prialnik et al., 2004, Fray and Schmitt, 2009), it would take ~4×10^{28} molecules/s (~10^3 kg/s) subliming (close to the typical activity level for an inner system SP comet near perihelion) to match the (0.7 W/m^2 * 6×10^8 m^2 surface area) of MU_{69} total input solar power. The mass of MU_{69} is about $(6 \times 10^8)^{3/2}$ m^3 * 500 kg/m^3 = 2×10^{15} kg. Since the 10^3 kg/s mass loss is always "on" for a body in a near-circular, stable orbit like MU_{69}'s, this means an MU_{69} consisting of solid N_2/CO would be fully sublimated in ~10^5 years, and any hypervolatiles providing substantive cooling would be quickly exhausted. (N.B. - The vast majority of small icy bodies known in the solar system are in such a hypervolatile-depleted condition. But one strong counter-example of an object temperature-controlled by apparent hypervolatile sublimation – that of comet C/2016 R2 – has been recently seen, and we discuss its case further in Section 5.5).

We can now go back to Eq. 3 and ask what the effect of any heating by short-lived radioactive elements like Al^{26} would be on our unit slab, and answer that they would offset the effects of any hypervolatile sublimative cooling by causing substantive heating in the first few Myr and reducing the timespan over which sublimative cooling can keep the object below Local Thermodynamic Equilibrium (LTE). The short-lived radionuclides are especially efficient at doing this deep inside the KBO through additional volume radioactive heating decay and thermal conduction terms on the left-hand side of Eq. 3 (Prialnik et al., 2004, 2006).

We are thus back to safely ignoring the effects of sublimative cooling
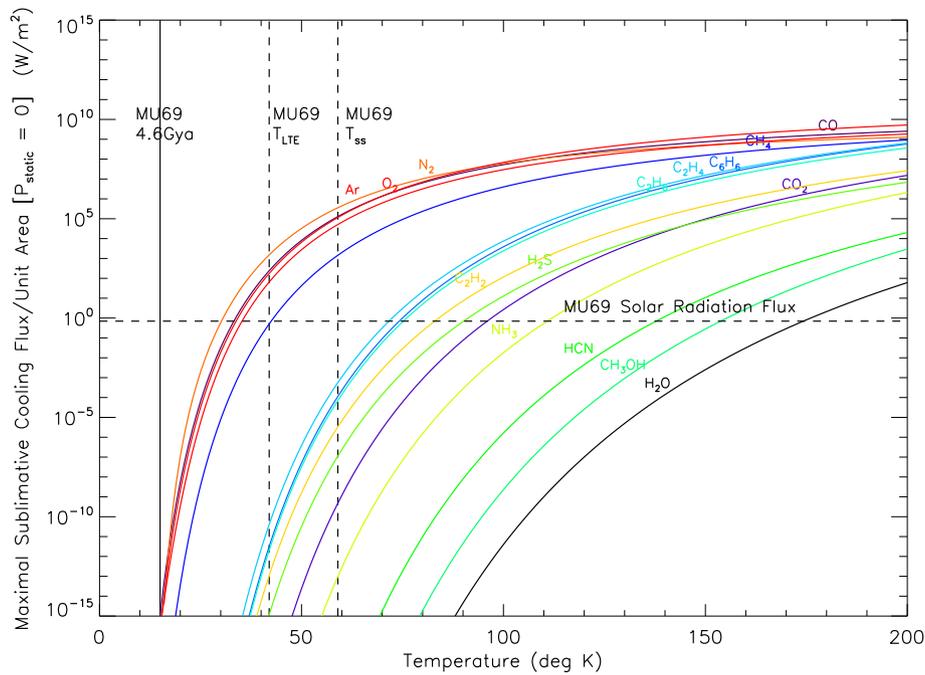
Fig. 4. Plot of the maximal possible sublimative cooling power per unit surface area for a given ice species vs. ambient temperature, assuming the ice species is uniformly distributed across MU$_{69}$'s sunlit side. Only for the hypervolatile species (N$_2$, CO, O$_2$, Ar, or CH$_4$) does the sublimative power achieve or exceed the input insolation power.

on timescales of >1 Myr, and with this zeroth-order approximation can produce a plot like that shown in Fig. 5. The same general family-of-curves shape is apparent in Fig. 5 as for the Q$_{gas}$ production rates in Fig. 3, but we have now added dashed horizontal lines at the Q$_{gas}$ rates that would deplete molar quantities (10^{19}/m^2 worth) of an ice species in 1 Yr, 1 Kyr, 1 Myr, and 4.6 Gyrs.

How to interpret this for an object like MU69? Also on Fig. 5 are 3 vertical lines, set at the T ~ 15 K of deep galactic ISM space; at the T$_{LTE}$ value of 42 K; and at the T$_{ss}$ value of 59 K. To 0th order, without

performing a detailed thermophysical model, once the hypervolatiles are gone, each portion of the surface will experience a temperature ranging from 15 to 59 K over an orbit, with an average T$_{LTE}$ of 42 K. The deepest interior regions, after the heat pulse from the short-lived radio-nuclides has dissipated and the insolation-driven thermal waves have stabilized, reaches a temperature half-way between the nightside and dayside temperature extremes of 15 and 59 K imposed by MU$_{69}$'s orbit and spin axis orientation, or ~ 37 K. Applying these temperature regimes to Fig. 5, it is seen that near the surface, the hypervolatile and
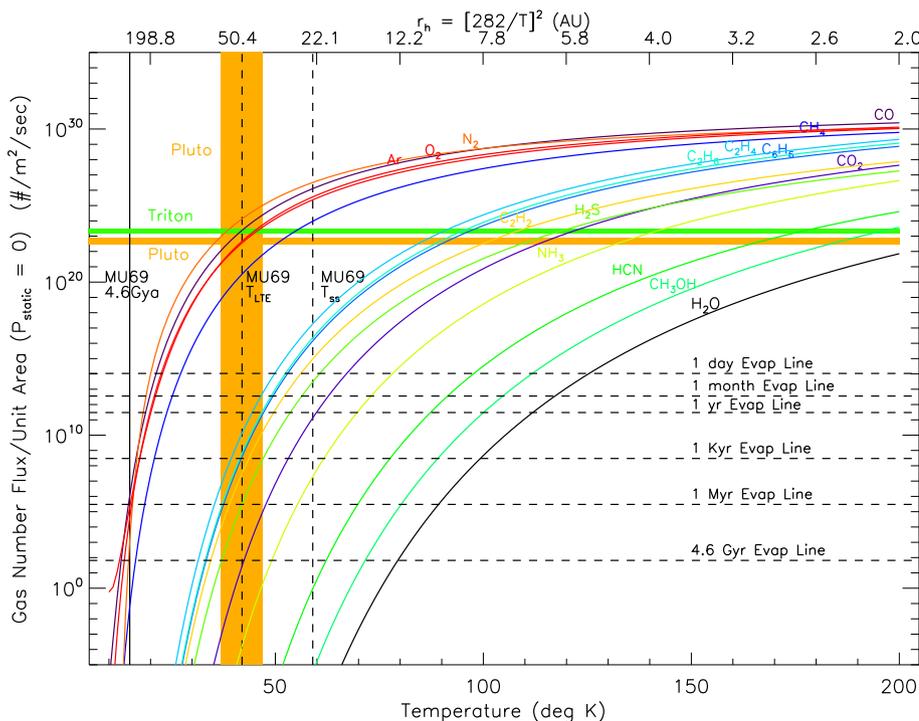
Fig. 5. Plot of Q$_{gas}$, the production rate of gas molecules for a given ice species, vs. ambient temperature, for a patch of unit surface area. This plot is useful in comparing to the molar surface density of an ice, ~10^{15}/cm^2 (=10^{19}/m^2). For an assumed time interval over which this outgassing occurs (e.g., 10^3 yrs. (=3×10^{10} sec), 10^6 yrs. (= 3×10^{13} sec), or 10^9 yrs. (= 3×10^{16} sec)), the maximal Q$_{gas}$ for which any appreciable solid ice remains (rather than sublimating) can be calculated (dashed horizontal lines). While this line of analysis involves assuming constant levels of gas mass loss over large periods of time, we have assumed the lowest possible loss rates (thermal only) and the method produces much more stringent limits on the possible presence of any ices. As a result, it immediately shows that only the highly refractory hydrogen-cross bonded ices (NH$_3$, HCN, CH$_3$OH, H$_2$O) can be present for a surface at today's sunlit value of T = ~40 K, and that any N$_2$, CO, O$_2$, Ar, or CH$_4$ ice incorporated by MU$_{69}$ when it first formed cold (at T ~ 15 K) in the optically dense mid-plane of the solar system's proto-planetary disk (PPD) was removed within ~1 Myrs of the mid-plane clearing and MU$_{69}$ warming up to ~40 K.

mid-volatile (C_2H_2, C_2H_6, H_2S, etc.) ices are removed within ~1 Myr and that CO_2 ice is removed on the order of 4.6 Gyrs, the age of the Solar System. A stronger, mildly hydrogen-bonded ice like NH_3 is moderately stable, or meta-stable, versus sublimation over 4.6 Gyrs (but will be removed by additional energy inputs above solar, see next Section 4.2). Strongly hydrogen-bonded "refractory" ices (HCN, CH_3OH, and H_2O) should be thermally stable over the 4.6 Gyr age of the Solar System. For the deepest interior regions, refractory (HCN, CH_3OH, and H_2O) ices should be stable over 4.6 Gyrs, and possibly NH_3 and CO_2 ice as well.

4.2. Lower limits to outgassing rate & surface re-processing

At this point we remind the reader that the mass loss rates plotted in Fig. 5 are lower bounding limits produced by insolative heating only. Any sort of effects that could cause increased loss – be they initial burdens of short-lived radioactive elements like Al^{26} in the first 10^7 yrs. of the early Solar System; Gyrs long-term surface sputtering by photons, solar wind particles, galactic cosmic rays (GCRs), or micrometeorites; passage of the subsolar point over the surface, raising the local temperature from T_{LTE} to $T_{subsolar}$, or from 42 to 59 K; or transient heating due to passing nearby O/B stars or nearby supernovae explosions every 10^8–10^9 yrs. (Stern, 2003) – will only increase the ice loss rate, making the on-the-cusp metastable ices unstable as well. We thus expect CO_2 and NH_3, marginally stable even when neglecting these processes, to be unstable on MU_{69}'s surface, leaving HCN, CH_3OH, and H_2O as the only ices to be present on the surface of MU_{69} on 01 Jan 2019 during the NH flyby.

More needs to be said about this. Given the solar system abundance of early short-lived radioactive elements like ^{10}Be, ^{26}Al, and ^{41}Ca estimated from chondritic meteorites (Thrane et al., 2006; Castillo-Rogez et al., 2007; Krot et al., 2012; Tang and Dauphas, 2015), the models by Choi et al., 2002, Merk and Prialnik, 2006, and Gounelle et al., 2008 argue for high central heating and material re-processing of the core of MU_{69} in the first few Myr due to the decay of such short-lived radionuclides (even melting in some cases, as the melting point of CH_3OH-H_2O ice can be as low as 157 K at the eutectic composition of 80 mol% CH_3OH; Miller and Carpenter, 1964). This is consistent with formation of MU_{69} by the streaming instability, currently understood as the likeliest accretional scenario for dynamically cold classical EKB objects (Nesvorný et al., 2019), i.e. way before dissipation of the protoplanetary gas after 5–10 Myr or ~ 10 ^{26}Al half-lives of 0.7 Myr. The surface of MU_{69}, however, only experienced low amounts of surface heating & reprocessing due to the poor thermal conductivity of the body and the short timespan of the radioactive decay input. The presence at the surface today of CH_3OH, a species that (although unreactive on experimental timescales) is not thermodynamically stable in liquid water over Myr (Shock and McKinnon, 1993), is an observational confirmation that any near-surface melting was likely limited in extent and in time. Observations of currently extant exo-PPDs (e.g., Anderl et al., 2016; Öberg et al., 2017; Loomis et al., 2020) and models of the solar nebula and PPDs around Sun-like stars (e.g., Lesniak and Desch, 2011; Krijt et al., 2018, 2020; Mousis et al., 2019) have mid-plane temperatures at 45 AU from the Sun at T ~ 15 to 25 K within the first few Myr of the solar system's existence. So at its birth in an optically thick region of the solar proto-planetary disk, the surface of MU_{69} was thus likely the coldest region of the body, with T ~ 15 to 25 K, capable of freezing out and maintaining hypervolatile ice phases (Fig. 5).

Once the short-lived radionuclides decayed and the PPD cleared, allowing direct insolation at MU_{69}'s location within the first ~10 Myr of the solar system's existence (i.e., "when morning arrived in the EKB"), MU_{69}'s subsolar surface rapidly warmed to ~50–60 K. This would have caused rapid sublimation of the surface hypervolatile ices (Figs. 4 & 5) and near-surface mass loss, which may be evidenced by the pit chains seen on MU_{69}'s limb (Stern et al., 2019; Spencer et al., 2020; Schenk et al., 2020) as well as by possible instances of scarp retreat seen on the small lobe (Moore et al., 2019). Other structures on

MU_{69}, like the rumpled surface texture and the delineated joints between apparent subunits on the larger lobe, could also be due to significant subsurface mass wasting "deflation" of its initial structure (Spencer et al., 2020, Schenk et al., 2020). The local temperature would have fallen from this peak towards ~40 K as the Sun finished its gravitational condensation and commenced nuclear fusion burning, appearing on the main sequence within the first ~100 Myr.

Over the next ~4 Gyr, the Sun would have been a consistent heat source for MU_{69}, although the environment at ~45 AU was likely subjected to a variety of other time-dependent energetic processes. Every 10^8–10^9 yrs., the transient effects of nearby passing O/B stars and supernovae acting on 10^1–10^3 yr timescales may have dramatically heated MU_{69}'s surface down to 10's of meters (Stern, 2003), removing all but the most refractory of ices (Fig. 5). This refreshed and modified surface will also have been dosed by photons (down to μm depths), solar wind particles (down to cm), micrometeorites (down to dm), and galactic cosmic rays (down to m) to create the optical surface we see today. We can thus expect that the optical surface of MU_{69} observed with New Horizons is likely only 10^8–10^9 yrs. old, having been processed by irradiation and micrometeorite bombardment. Since the colored surfaces of both lobes appeared to be compositionally very uniform to New Horizons (Stern et al., 2019; Grundy et al., 2020), we can infer that both lobes were compositionally uniform and similar to begin with.

As evidence of potential surface radiolytic effects, it is worth noting that the spectral signature of CH_3OH in the wavelength region in which it was detected with New Horizons (Fig. 1) is subject to subtle modification by radiation processing. Specifically, while the stronger 2.27-μm band is fairly durable against radiation, the weaker band at 2.34 μm is not. Brunetto et al. (2005) irradiated films of frozen CH_3OH and water-methanol (1:1) with 30 keV He^+ and 200 keV H^+ ions. The 2.27-μm band decreased slightly in strength, but the 2.34-μm band eventually disappeared, and new bands at 2.321, 2.355, and 2.37 μm appeared. New molecular bands of CO and CH_4 appeared as a result of the irradiation of the methanol-water mix with a dose of 28 eV/16 amu with the 30 keV He^+ ions. In the New Horizons LEISA flyby spectrum, the random noise level in the wavelength region of the weaker CH_3OH bands does not allow us to discriminate between unprocessed and processed CH_3OH. We note, however, that the original analysis of the spectrum of 5145 Pholus (Cruikshank et al., 1998) yielded a good match with CH_3OH (prior to availability of the Brunetto et al., 2005 work) and more recent examination of the Pholus spectrum shows, within the constraints of the random noise level, that it is more consistent with the spectrum of old, irradiated CH_3OH than it is with pristine CH_3OH in terms of the three new bands that Brunetto et al. found.

4.3. One species not well modeled - H_2CO (formaldehyde) ice

As a first product of CO hydrogenation (via H-atom additions) on the way to forming methanol, formaldehyde is a potentially important ice in the makeup of MU_{69}. It is also a major radiation degradation product of CH_3OH (Allamandola et al., 1988; Schutte et al., 1993b). However, the stability of its solid phase ice is difficult to gauge from the extant literature. To quote Fray and Schmitt, 2009, "The triple point of H_2CO is located at 155.1 ± 0.3 K, but its pressure is unknown (Table 2). From the data of Spence and Wild (1935), concerning the evaporation equilibrium, we can estimate that the pressure at the triple point is about (4 ± 1) x 10^{-4} bar. Lide (2006) reports data only for the evaporation equilibrium. No experimental data concerning the sublimation equilibrium have been found"

Comparative values for methanol are a triple point at 175.5 ± 0.5 K and pressure about (1.8 ± 0.2) x 10^{-6} bar, implying that formaldehyde is 200 times more volatile at 20 K lower temperature. Cervinka and Fulem (2017) quote theoretical values for H_{subl} of formaldehyde of 24.4 kJ/mol at 0 K and 26.3 kJ/mol at 155 K, but these are much smaller than the 34.2 ± 1.5 kJ/mol they list as the experimental measure of H_{subl} at 155 K, and in all other cases their calculations have either matched

experimental values or fallen under them by up to 100%. We thus adopt, with caution, a value for H_{subl} closer to 34 kJ/mol for determining its P_{sat} behavior, and note that this is close to the value of H_{subl} for NH_3. Constructing a $P_{sat} = A*e^{(-B/T)}$ curve with $H_{subl} = 34$ kJ/mol and anchored point at 40 Pa and 155 K in Fig. 2, we also find a curve similar to that of NH_3. (The triple point (T,P) values of (195.4 K, 0.061 bar) listed by Fray and Schmitt, 2009 for NH_3 fall nicely on its P_{sat} curve in Fig. 2, giving us confidence in this line of reasoning.) *We therefore infer that H_2CO in its pure ice form will have thermal meta-stability over the age of the solar system similar to NH_3.* This is consistent with its ability to form weak, but finite hydrogen bonds between the carbonyl oxygen and an adjacent aliphatic hydrogen.

One of the difficulties in establishing the sublimation temperature of H_2CO is likely due to the fact that it is highly reactive even at temperatures as low as 40 K (Schutte et al., 1993a, 1993b). In pure form it can polymerize into polyoxymethylene (paraformaldehyde) and if other species like H_2O, NH_3 and CH_3OH are present, it can polymerize to form a host of compounds having polyoxymethylene backbones with some H atoms substituted for by other functional groups like -NH_2, -CH_3, and -OH (Schutte et al., 1993b). H_2CO is also known to easily cross-link via ion-radical and photon-induced polymerization. Once polymerized, H_2CO is no longer present as a lightweight molecule but is instead associated with structures having much higher molecular weights, i.e., it is no longer a simple ice component, but is instead a complex macromolecule. In this macromolecular form the H_2CO moiety is expected to be very thermally stable vs. sublimation. Polymerized H_2CO could be stored in KBOs and their cometary descendants in this form and would not be expected to be released until exposed to very high temperature excursions (T > 300 K) during inner system passages (e.g. Fray et al., 2004).

5. Implications and predictions

In the above sections, we presented the results of simple thermodynamic calculations for the stability and lifetime of different ice species on the cold classical KBO body MU_{69}. The results for a flattened, 4.6 Gyr old KBO like MU_{69}, with obliquity near 90° and spinning around its short axis in a stable $r_h = 45$ AU orbit suggest that only the refractory strongly hydrogen bonded ices (H_2O, CH_3OH, and HCN, and poly-H_2CO) should have remained stable throughout until the present day. The somewhat less refractory and more volatile species NH_3 and CO_2 could possibly also exist in the cooler "deep interior regions", if further detailed modeling (including realistic ranges of hypervolatiles, short-lived radioactives, and initial temperature conditions) bears out their survival past the first few Myr. All other ice species, especially the hypervolatiles (N_2, CO, CH_4, Ar, etc.) should be long gone. *The importance of refractory hydrogen bonded species like methanol ice in outer solar system bodies is a relatively new concept, as is the rapid removal of hypervolatile ices.* In this section we discuss how these results fit into the bigger picture of other KBOs, the Pluto System, and of the KBOs' dynamical descendants, the Centaurs and Short Period (SP) comets.

5.1. KBOs to Centaurs to Comets

To begin with, we present the state of current observational knowledge of ices on the KBOs, Centaurs, and SP comets. Water and methanol ice, but also ofttimes ammonia and the hypervolatile ices, are known to be present on the largest KBOs (Barucci et al., 2008, 2011; Brown et al. 2011; Brown, 2012). By contrast, the Centaurs show absorptions only due to water ice and methanol (for a few of the most distant objects; in fact the first detection of methanol on a small icy solar system body was

for Centaur 5145 Pholus by Cruikshank et al., 1998). Correlations of the outgassing activity of 23 Centaurs with their perihelion distance from the Sun led Jewitt (2009) to conclude that the activity of the inner ($r_h < 10$ AU) Centaurs is driven not by CO or CO_2 ice sublimation, but instead by crystallization of amorphous water ice and the "squeezing out" of trapped molecules no longer able to fit into the reduced lattice pore space of the newly crystallized ice. SP comet surface spectra do not show any obvious absorption features due to abundant ices, except for the rare small patch of water ice (Sunshine et al., 2006; Quirico et al., 2015, 2016; Lisse et al., 2017). However, their comae, produced largely by water ice sublimation, show an abundant range of icy species (Bockelée-Morvan et al., 2004, Mumma and Charnley, 2011) with most species on the order of 0.1–1.0% of the H_2O gas abundance, with the exception of CO (0.5–25%), CO_2 (2–12%), and CH_3OH (0.5–5.0%) at total relative abundance [CO + CO_2 + CH_3OH] ~ 20% (A'Hearn et al., 2012).

Given these observational facts, how do we make evolutionary sense of them? *Firstly,* we note that the hypervolatiles CO, N_2, and CH_4 are commonly present and abundant on the largest KBOs, as well as in the giant planets and their moons – yet our calculations above show (Figs. 4 & 5) that if they were ever incorporated into an MU_{69}-sized, near zero-gravity body, they were stably bound at EKB temperatures for less than 1 Myr. *This immediately implies that if these largest EKB bodies formed from small KBOs or the same material as smaller KBOs, then (1) they did so within 1 Myr of the PPD mid-plane clearing; or (2) that there was abundant CO, N_2, and CH_4 gas in the PPD when they became large enough to gravitationally bind these species; or (3) that they are all melted and differentiated through and through, and the surface hyper-volatile ices are the result of concentrating the small remnants of the hypervolatiles contained in bulk refractory water phases onto the surface* (Glein and Waite 2018).

All 3 of these Pluto formation scenarios are very plausible given current understanding, and all 3 cases provide important constraints that can be tested and modeled. For instance, in the first two cases, the large hypervolatile-rich bodies have to have formed quickly, via streaming instability/pebble accretion/bottom-up aggregation, within the first few Myr of the Solar System. In the case of Pluto and Charon, this is consistent with the 4 Gyr + cratering ages found on their surfaces by New Horizons (Robbins et al., 2019; Singer et al., 2019), and with streaming instability + gravitational instability models of EKB planetesimal formation (McKinnon et al., 2020) or pebble accretion (Nesvorný et al. 2010, 2019; Lambrechts and Morbidelli, 2016) in a pre-migration EKB region of the PPD hundreds of times more massive than today. In the third case, as proposed by Glein and Waite (2018), Pluto and Charon would have to be highly differentiated in their interiors; McKinnon et al., 2017 argued that differentiated interiors are likely for them from the lack of compressional geological features (and thus the lack of a run of higher and higher density ice phases) seen on the two bodies, while Weaver et al. (2016) argued for differentiated proto-Pluto and proto-Charons due to the highly icy nature, and thus highly differentiated nature, of the system's smallest moons, assuming these moons formed during the Pluto-Charon binary-forming impact.

On the other hand, the N_2/CO >> 1 ice abundance ratio found on Pluto's surface (Grundy et al., 2016; Protopapa et al., 2017; Schmitt et al., 2017) is counter to the N_2/CO ~ 0.10 abundance ratio expected for these ices trapped in water ice phases; CO with its small but finite dipole moment is much more efficiently trapped in polar water ice than homonuclear, zero dipole N_2 from a starting equal mix of the two gases (Yokochi et al., 2012; K. Öberg 2019, priv. Commun.). However, Kamata et al. (2019) argue to the contrary that differential N_2 versus CO trapping ability being the case, geochemical and geophysical mechanisms at work on a Pluto surface-devolatilized by a Charon forming impact (and

subsequently re-volatilized from deep interior stores of hypervolatiles) could allow for N_2 re-concentration versus CO on its surface.

5.2. No "top-down" KBO formation

If we turn the problem around, and note that we do not see nebular abundances of N_2 and CO in the comets or small KBOs, this argues against these objects forming as large bodies and incorporating everything available in the PPD via gravity stabilization, then collisionally fragmenting and retaining these ices. The limits on MU_{69}'s density of 0.2–0.8 g/cm^3 (McKinnon et al., 2020), and the density values of $\sim$0.5 g/cm^3 for comet nuclei and the smaller KBOs vs the range of 1.5–2.3 g/cm^3 for the largest KBOs (Lacerda and Jewitt, 2007; Brown, 2013) also argue against a "top-down" KBO formation scenario. This conclusion is also consistent with the inference by Krivov & Wyatt (2020) that in order to solve the "debris disc mass problem", planetesimals in nearby exosystems with sun-like primary stars are likely born small.

5.3. Implications for methanol in the Pluto system

The moons of Pluto are on the same size scale as KBO MU_{69}, with somewhat lower expected ambient surface temperatures ($\sim$35 K) than MU69's, despite their being closer to the Sun by a factor of $\sim$45/35, mainly due to their very high albedos ($p_v = 0.4$ to 0.6 vs MU69's $p_v = 0.16$, Weaver et al., 2016). The resulting v_{escape} and $v_{thermal}$ values still clearly put them in the airless $P_{ambient} \approx 0$ regime (Section 2), and we can expect them to have lost all their hypervolatiles over the age of the solar system, assuming their recondensation and incorporation after the Charon-forming impact event that created them (Canup, 2005; McKinnon et al., 2017) was possible. On the other hand, methanol ice should be quite stable, as seen on MU_{69}, and it is possible the moons contain substantial amounts of it.

Similarly, we can expect Pluto and Charon to have large amounts of stable methanol ice content; methanol ice should be almost as strong and as stable as water ice on these bodies. If the primordial KBO methanol: water ratio is on the order of unity, as implied from the NH flyby of MU_{69}, then Pluto & Charon, with rock:ice ratios on the order of unity, should contain copious amounts of methanol "rock" in their interiors (and dissolved methanol in their subsurface oceans, if any exist) that need to be considered when modeling their geological structure and history. A search for exposed methanol ice in the NH LEISA data to verify this assertion is difficult on Pluto, however, due to the abundant methane ice coverage on its surface, as methane shares similar 1–2.5 μm absorption features to methanol.

5.4. Non-zero amounts of hypervolatiles observed in Comets

The fact that there are low, but finite amounts of hypervolatile species seen in SP comets derived from the EKB (Bockelee-Morvan et al. 2004, Mumma and Charnley 2011), implies that there must be some reservoir for them in these recent EKB escapees. The current crop of SP comets have been in the inner system for $<10^5$ yr (Levison and Duncan, 1994; Lisse, 2002), so their deep interiors are still warming from the recent increase in surface insolation (Benkhoff and Huebner, 1996; Huebner, 2002; Huebner et al., 2006) and the fate of any core ices will be dominated by the interior composition established 4.6 Gyr ago. However, our calculations above show that except for H_2O, CH_3OH, HCN, or polymerized H_2CO compounds, this reservoir cannot contain hypervolatile ice phases, *unless they have deeply buried regions held*

at $\sim$ 15 K since the beginning of the Solar System.

This is highly unlikely given that the models of Choi et al. 2001, Merk and Prialnik, 2006, and Prialnik 2009 show that KBO cores are always as warm or warmer than their surface; the lack of substantial hypervolatile emission from end member objects 45P/Honda-Mrkos-Pajdušáková, 46P/Wirtanen, and 103P/Hartley 2 (small comets near the end of their lives emitting chunks of their cores, A'Hearn et al., 2011, DiSanti et al., 2017); the lack of hypervolatile emission seen from the recently split comets 73P/SW3 (Dello Russo et al., 2007) and 17P/Holmes (Dello Russo et al., 2008); and the singularly unique behavior of the one truly hypervolatile dominated comet, Oort Cloud object C/2016 R2 (Pan-STARRS) (Biver et al., 2018, McKay et al., 2019; see below). Some authors, like Mousis et al., 2019, even argue that there were never any majority hypervolatile ices in small solar system bodies – they condensed directly out of the PPD as water ice dominated mixtures instead, and that impure crystalline water ice dominated, inner system icy small bodies were able to build the giant planets seen today.

We are thus left to follow Iro et al.'s, 2003 & Jewitt's, 2009 concept (now re-checked by Li et al., 2020's new outer Centaur activity survey) that the hypervolatiles and moderately-volatile species in the Centaurs and SP comets are protectively stored in H_2O ice matrices – first at high concentrations in cold (T < 80 K) amorphous water ice composites, then in lower concentrations in warmer T > 100 K crystalline water ice matrices limited by the maximum interlattice "pore space" trapping capability of the crystallite. This is consistent with the early work of Prialnik et al. (1987) who argued that the presence of amorphous ice within the subsurface of comets – inferred from observations of outgassing at surprisingly large heliocentric distances (5.8–11.4 AU) and attributed to the annealing of amorphous ice as comets first enter the inner Solar System (Bar-Nun et al., 1985; Prialnik and Bar-Nun, 1990; 1992; Jenniskens and Blake, 1996, Meech et al. 2009, Lisse et al., 2013) – provides a clear constraint on the maximum parent body temperatures (T < 135 K) experienced over comet lifetimes. It is also consistent with the newer work on mixed water ice phases of Guilbert-Lepoutre and Jewitt (2011), Marboeuf & Schmitt (2014), and Guilbert-Lepoutre et al. (2016) motivated by ROSETTA studies of comet 67P/Churyumov-Gerasimenko.

H_2O ice reservoirs for remnant icy molecules also explain the seeming disconnect between the strong CH_3OH vs H_2O signature on the surface of MU_{69}, the weak CH_3OH:H_2O signature of several Centaurs, and the low CH_3OH:H_2O abundance ratio seen in the atmospheres of the active SP comets. Any CH_3OH (and maybe HCN) ice phases that are stable at MU_{69}'s T = 42 K temperature in the heart of the EKB sublimes within the few Myrs of time it takes to scatter the KBO past Neptune ($r_h \sim 30$ AU, T $\sim$ 51 K), then Uranus ($r_h \sim 19$ AU, T $\sim$ 64 K), and into Saturn's dynamical regime ($r_h \sim 9.6$ AU, T $\sim$ 91 K; Fig. 4). What is left after this process are the molecules mixed in with H_2O ice, and subject to any changes in the state of the H_2O ice, like the amorphous - > crystalline water ice transitions at T = 80–120 K (Blake et al., 1991), and water ice sublimation at T > 140 K (Sandford & Allamandola 1993b). (Note that both of these processes proceed at a temperature-dependent rate; Schmitt et al. (1989) gives the timescale for the amorphous - > crystalline water ice transition as $\tau = (3 \times 10^{-21}$ yrs) * exp(E_a/kT) with E_a/k = 5370 K, and we show the rate of water ice sublimation/unit area vs temperature in Fig. 3. Also note that the inter-lattice volume of crystalline H_2O ice can only hold up to $\sim$17% CO_2 or $\sim$ 20% CO by number, similar to the maximum abundances seen in comets for these species [Bockelee-Morvan et al. 2004].)

This line of reasoning would be bolstered by a new, improved telescopic survey of the Centaur population to study the pattern of CH_3OH

ice presence vs. heliocentric distance; if correct, then abundant CH_3OH ice should exist only in the outer, more distant and inactive Centaurs. In summary, KBOs like MU69 should be much richer in amorphous water ice and its associated minority ice impurities (like the hypervolatiles, NH_3, and CO_2), as well as the other stable refractory hydrogen bonded ices (CH_3OH, HCN), than SP inner system comets dominated by crystalline water ice phases + impurities.

The presence of water ice reservoirs for remnant volatile ice molecules also makes a strong prediction about Q_{gas}, the gas production trends for comets. Species that are sourced from amorphous water ice composites do not need to track Q_{water}, only the rate at which amorphous water ice crystallizes to produce solid crystalline water + gaseous minor species. Amorphous water ice minor species can also be present in much greater numbers vs water than the limited amount ($\sim$20%) possibly carried in the pore spaces of cubic crystalline water, i.e., as H_2O ices warm through $\sim$80 K, the rearrangement of H_2O molecules during the conversion of H_2O from one amorphous phase to another will allow some hypervolatiles to escape (Sandford and Allamandola, 1988, 1990; Blake et al., 1991). Additional hypervolatile loss can occur when the ice is warmed to temperatures that convert the amorphous H_2O ice to its cubic crystalline form (Schmitt et al., 1989, Jenneskins & Blake 1996)[4] It is only upon subsequent sublimation of the cubic crystalline H_2O (as seen for comets inside 3 AU) that the emission rate of remaining ($\sim$20% total vs water) minority volatiles will track Q_{water}.

5.5. C/2016 R2 (PANSTARRS)

Our physical model for MU$_{69}$'s and Pluto's ices has something to add to the discussion of the recently discovered, highly unusual comet C/2016 R2 (PANSTARRS) (hereafter R2). This is a dynamically old Oort Cloud comet ($P_{orbit} \sim$ 20,000 yrs) exhibiting a highly unusual coma gas composition. It outgasses CO, N_2, CH_4, and CH_3OH at extremely high rates compared to its minuscule to nonexistent water gas emission rate (Biver et al., 2018; McKay et al., 2019). Its effective radius of $\sim$15 km (or less; McKay et al., 2019) is comparable to that of MU$_{69}$, but much smaller than any of the KBOs able to gravitationally retain hypervolatile ices. By all coma gas abundance standards, this comet is acting like a piece of *thermally unprocessed* KBO that has only recently been warmed up past the methanol ice sublimation temperature. Given the Q_{gas} curves of Fig. 5, we could then suppose it was formed at T < 20 K in an optically thick mid-plane region, then ejected into the Oort Cloud to stay at these temperatures until very recently, when it was perturbed onto the orbit we currently see today - where it is undergoing intense sublimation of its hypervolatiles, which as we saw in Section 4.1 is enough to sublimatively cool the body to very low temperatures where water ice is rock-like and inactive sublimation-wise.

Is this a viable picture? It takes a major dynamical event to put an object onto an Oort Cloud orbit. KBO-KBO collisions, like the Haumea

family formation event or the Pluto-Charon formation event, cannot do this as Pluto's escape velocity (v_{esc}) and EKB relative velocities are too low (Canup, 2005; Stern et al., 2006; Sekine et al., 2017). Dynamical scattering by a giant planet with a large v_{esc}, as in the initial phases of planetary core formation via planetesimal-aggregation, or during proto-Neptune's later migration through the inner proto-EKB, can do this.[5] The latter case would require Neptune's migration through the inner proto-EKB to have occurred no more than a few Myr after the midplane clears for R2's hypervolatiles to have remained stable (Section 4), contrary to the early Nice models (e.g. Gomes et al. 2005), but consistent with later Nice scenarios including ejected outer planets (e.g. Nesvorný and Morbidelli, 2012).

For the sake of completeness, another possibility, that R2 somehow retained significant deep interior hypervolatiles in the inner solar system until being scattered into the Oort Cloud, should also be entertained. Following the work of Choi et al. 2001, Merk and Prialnik, 2006, and Prialnik 2009, this would require an unusually large overabundance of initial hypervolatiles and/or underabundance of short-lived radionuclides. While this seems very unlikely, given the evidence on hypervolatile-devoid comet interior composition we have from observations of end member objects 45P/Honda-Mrkos-Pajdušáková, 46P/Wirtanen, and 103P/Hartley 2 (small comets near the end of their lives emitting chunks of their cores, A'Hearn et al., 2011, DiSanti et al., 2017); the lack of hypervolatile emission seen from the recently split comets 73P/SW3 (Dello Russo et al., 2007) and 17P/(Dello Russo et al., 2008), and the hypervolatile-devoid KBO compositions discussed in this paper, it is perhaps possible that this likelihood is no less extreme than requiring an object to be scattered into the Oort Cloud during the era of giant planet formation/migration. Further modeling work will be required to assess the relative likelihoods of these two scenarios.

In summary, we find that in the ice-sense, MU$_{69}$ is "more primordial" than SP comets, and as or more primitive as the most distant and inactive Centaurs, like 54598 Bienor (orbit semimajor axis a = 16.5 AU), 5145 Pholus (a = 20.3 AU), and 52975 Cyllarus (a = 26.2 AU). By contrast, MU$_{69}$, like other small KBOs, has not retained much of the PPD hypervolatile ice species found on the largest KBOs, the unique Oort Cloud comet C/2016 R2 (PANSTARRS), and in the giant planets and their moons, as it was unable to gravitationally bind them versus their thermal instability in the present Edgeworth-Kuiper Belt. What it does contain of these species is likely bound up as minor impurities in more thermally stable water ice phases.

---

[4] However, if there is sufficient CH_3OH present to force enclathration at $\sim$120 K, ice loss behavior is more complicated. Conversion to a clathrate will allow the ice to accommodate $\sim$7% CH_3OH relative to H_2O and a combined total of $\sim$14% of other volatile species within the clathrate structure; excess amounts of CH_3OH and other volatiles present will be squeezed out of the clathrate. The resulting phase transition forms a porous clathrate structure from which the excess CH_3OH and other molecules can rapidly sublime (Blake et al., 1991). This would result in a 'burst' of emitted CH_3OH and other more volatile species, with the released amounts of each being determined by their excess abundances over that which could be accommodated by the clathrate. Once again, the loss of these volatiles would not track Q_{water}, although if excess CH_3OH is present during enclathration, they might track $Q_{methanol}$ for the duration of the 'burst'. After enclathration all the remaining volatiles will be trapped in, and controlled by, the clathrate structure and will be unable to leave until the H_2O clathrate structure sublimes. At this point, the loss of other volatiles would be expected to closely track Q_{water} and be constrained to abundance ratios capped by the clathrate structure.

[5] The main issue with this picture is how many times R2 can pass through perihelion and still remain stable against evaporative disintegration. A 15 km radius object of $\sim$0.5 g/cm^3 density masses on the order of 7×10^{15} kg. At the $Q_{gas} \sim 10^{29}$ molecules/s outgassing levels seen during R2's current apparition for its current perihelion distance of 2.6 AU it will lose $\sim 3 \times 10^7$ s [1 yr]* (28 amu for CO/N$_2$*1.67 $\times 10^{-27}$ kg/amu)*1 $\times 10^{29}$ molecules/s $\sim 1 \times 10^{11}$ kg. Thus it should be able to endure $\sim 7 \times 10^4$ more of these kind of passages before dissipating, which should take $\sim 2 \times 10^4$ yrs./passage * 7×10^4 passages = 1.4×10^9 yrs., or 1.4 Gyrs. It is thus unlikely to have been on its present orbit for more than 1 Gyr. Note that a 10^{29} molecules/s level of hypervolatile outgassing is reasonable, and can be supported by a 15 km radius object that is losing molar amounts of ice surface every second: $(2*pi*r^2$ cm$^2)*(2 \times 10^{15}/$cm^2/s$) = 3 \times 10^{28}$ mol/s. From section 4.1 and Tables 1 & 2, the evaporation of 1 mol of hypervolatile ice requires $\sim$7.3 kJ of heat, thus the amount of hypervolatile cooling from the emission rate of 10^{29} molecules/s = 1.6×10^5 mol/s is $\sim 1.4 \times 10^9$ J/s, the same order of magnitude, $(1-0.9) * \pi R_{nucleus}^2 * (0.1$ W/cm$^2 *$ $(1.0$ AU/2.6 AU$)^2) = 1 \times 10^{10}$ W, as the insolation heating of the Sun is delivering to R2's nucleus (with assumed albedo = 0.90) at 2.6 AU. So the observed mass loss rate of R2 being attributed to hypervolatile sublimation makes rough sense if R2 is feverishly sublimating from its entire sunlit surface during the small portion of each 20,000 yr long orbital cycle where it is intensely heated.

6. Conclusions

In this paper we have found, from simple thermodynamic arguments independent of detailed formation scenario assumptions (e.g., formation location in the proto-solar nebula or the PPD, amount of Al^{26} incorporated & when, interior detailed structure), that New Horizons should not have seen any typical cometary icy material on the surface of MU_{69} other than the highly refractory ices H_2O, CH_3OH, HCN, and poly-H_2CO. These are the maximal possible set for the current low-level insolation conditions. Any positive temperature excursions, due to nearby passing hot stars, nearby supernovae, impacts, meteorite gardening, etc. could only remove more ice, and reduce this possible set. The New Horizons science team has already announced the detection of CH_3OH and evidence for H_2O on this object (Lisse *et al.*, 2017, Stern *et al.* 2019, Grundy *et al.*, 2020). We predict that further absorption feature detections, if any, will be due to an HCN or poly-H_2CO based ice species. In having evidence for these additional non-water ice phases from the NH flyby spectral mapping of its surface, MU_{69} appears akin to the most distant inactive Centaurs like 54598 Bienor, 5145 Pholus and 52975 Cyllarus. Because of this last point, we suggest a new survey of the distant Centaur and small KBO populations to search for methanol ices.

Compared to an inner system SP comet dominated by crystalline ice phases with limited interlattice carrying volume for minor impurities, our thermal stability analysis suggests that KBOs like MU_{69} should be much richer in amorphous water ice and its associated minority ice impurities (like the hypervolatiles, NH_3, and CO_2), as well as the other stable refractory hydrogen bonded ices (CH_3OH, HCN). On the other hand, MU_{69} should have lost all of its original hypervolatile (CO, N_2, CH_4) majority ice phases, just as the SP comets have. Current models of our PPD, coupled with ALMA exo-PPD observations, lead us to the conclusion that MU_{69} "formed in the dark" in the EKB region, unable to see the nascent, variable, highly luminous YSO/TTauri Sun (Briceno et al., 2001; Thrane et al., 2006), in an optically thick mid-plane. It was thus able to initially incorporate hypervolatile ices at a local $T < 20\,K$, but that these were quickly lost from the body within the first 1–10 Myr due to the combined action of short-lived radionuclide decay and surface warming upon PPD mid-place clearing. By contrast, Pluto was able to retain its original primordial volatiles via gravitational capture into an exobase (Schaller and Brown, 2007). Finally, the advent of the uniquely hypervolatile-dominated object comet C/2016 R2 (Pan-STARRS) shows us what a truly primordial, hypervolatile ice rich object behaves like upon warming in the inner system. Its uniqueness compared to thousands of other comets is striking, and highlights what has not been seen in recently fragmented, split, or hyperactive near-dead cometary cores, nor in MU_{69} – evidence for deep down core hypervolatile ices. This leads us to conclude that comet R2 was likely placed onto an Oort Cloud orbit very quickly after its formation in the optically thick PPD mid-plane, by scattering from a nascent giant planet or by proto-Neptune as it was migrating.

Declaration of Competing Interest

None.

Acknowledgements

Appendix A. Supplementary data

Supplementary data to this article can be found online at https://doi.org/10.1016/j.icarus.2020.114072.

References

A'Hearn, M.F., et al., 2011. Science 332, 1396.

A'Hearn, M.F., Feaga, L.M., Keller, H.U., et al., 2012. Astrophys. J. 758, 29.

Allamandola, L.J., Sandford, S.A., Valero, G., 1988. Icarus 76, 225.

Allamandola, L.J., Sandford, S.A., Tielens, A.G.G.M., Herbst, T.M., 1992. Astrophys. J. 399, 134.

Anderl, S., Maret, S., Cabrit, S., et al., 2016. Astron. Astrophys. 591. A3 CO/CH3OH snow lines.

Bar-Nun, A., Herman, G., Rappaport, M.L., Laufer, D., 1985. Icarus 63, 317–332.

Bar-Nun, A., Dror, J., Kochavi, E., Laufer, D., 1987. Phys. Rev. B 35, 2427.

Barucci, M.A., Brown, M.E., Emery, J.P., Merlin, F., 2008. Composition and Surface Properties of Transneptunian Objects and Centaurs. In: Barucci, M.A., Boehnhardt, H., Cruikshank, D.P., Morbidelli, A. (Eds.), The Solar System Beyond Neptune, 143–160.

Barucci, M.A., Alvarez-Candal, A., Merlin, F., Belskaya, I.N., de Bergh, C., et al., 2011. Icarus 214, 297–307.

Benkhoff, J., Huebner, W.F., 1996. Planet. Space Sci. 44, 1005–1013.

Bertrand, T., et al., 2019. Icarus 329, 148–165.

Bieler, A., et al., 2015. Nature 526, 678–681.

Biver, N., et al., 2018. Astron. Astrophys. 619, A127.

Blake, D., Allamandola, L., Sandford, S., Hudgins, D., Freund, F., 1991. Science 254, 548–551.

Bockelée-Morvan, D., Crovisier, J., Mumma, M.J., Weaver, H.A., 2004. The composition of cometary volatiles. In: Festou, M.C., Keller, H.U., Weaver, H.A. (Eds.), Comets II, 745. University of Arizona Press, Tucson, pp. 391–423.

Briceno, C., et al., 2001. Science 291, 93.

Brown, M.E., 2012. Annu. Rev. Earth Planet. Sci. 40, 467–494.

Brown, M.E., 2013. Astrophys. J Lett 778, 2.

Brown, M. E., Burgasser, A. J. & Fraser, W.C. 2011, "The surface composition of large kuiper belt object 2007 OR10", Astrophys. J. 738, L26.

Brunetto, R., Baratta, G.A., Domingo, M., Strazzulla, G., 2005. Icarus 174, 226–232.

Canup, R.M., 2005. Science 307, 546–550.

Castillo-Rogez, J.C., Matson, D.L., Sotin, C., et al., 2007. Icarus 190, 179.

Catling, D.C., Zahnle, K.J., 2009. SciAm 300, 36.

Catling, D.C., Zahnle, K.J., 2017. Astrophys. J. 843, 122.

Červinka, Fulem, 2017. J. Chem. Theor. Comput. 13, 2840–2850.

Choi, Y.-J., Cohen, M., Merk, R., Prialnik, D., 2002. Icarus 160, 300–312.

Cruikshank, D.P., Roush, T.L., Bartholomew, M.J., et al., 1998. Icarus 135, 389–407.

Dello Russo, N., Vervack Jr., R.J., Weaver, H.A., et al., 2007. Nature 448, 172.

Dello Russo, N., Vervack Jr., R.J., Weaver, H.A., et al., 2008. Astrophys. J. 680, 793.

DiSanti, M.A., Bonev, B.P., Dello-Russo, N., et al., 2017. Astron. J. 154, 246.

Earle, A., et al., 2017. Icarus 287, 37–46.

Fray, N., Schmitt, B., 2009. Planet. Space Sci. 57, 2053–2080.

Fray, N., Be'nilan, Y., Cottin, H., Gazeau, M.-C., 2004. JGR 109, E07S12.

Gladstone, G.R., et al., 2016. Science 351, 8866.

Glein, C.R., Waite, J.H., 2018. Icarus 313, 79–92.

Gounelle, M., Morbidelli, A., Bland, P.A., et al., 2008. Meteorites from the outer solar system? In: Barucci, M.A., Boehnhardt, H., Cruikshank, D.P., Morbidelli, A. (Eds.), The Solar System Beyond Neptune, 592. University of Arizona Press, Tucson, pp. 525–541.

Grundy, W.M., et al., 2016. Science 351, 9189.

Grundy, W.M., Bird, M.K., Britt, M.K., T, D., et al., 2020. Science 367 eaay3705.

Guilbert-Lepoutre, A., Jewitt, D., 2011. Astrophys. J. 743, 31.

Guilbert-Lepoutre, A., Rosenberg, E.D., Prialnik, D., Besse, S., 2016. MNRAS 462, S146–S155.

Huebner, W.F., 2002. Earth Moon Planets 89, 179–195.

Huebner, W.F., Benkhoff, J., Capria, M.-T., et al. 2006 "Heat and gas diffusion in comet nuclei", SR-004, ISBN 1608-280X. Published for the International Space Science Institute, Bern, Switzerland, by ESA Publications Division, Noordwijk, The Netherlands, June 2006.

Iro, N., Gautier, D., Hersant, F., Bockelée-Morvan, D., Lunine, J., 2003. Icarus 161, 511–532.

Jenniskens, P., Blake, D.F., 1996. Astrophys. J. 473, 1104.

Jewitt, D.C., 2009. Astron. J. 137, 4296–4312.

Krijt, S., Schwarz, K.R., Bergin, E.A., Ciesla, F.J., 2018. Astrophys. J. 864, 78.

Krijt, S., Bosman, A.D., Zhang, K., et al., 2020. CO Depletion in Protoplanetary Disks: A Unified Picture Combining Physical Sequestration and Chemical Processing. arXiv:2007.09517.

Krot, A.N., Makide, K., Nagashima, K., et al., 2012. Meteorit. Planet. Sci. 47, 1948–1979.

Krivov, A.C., Wyatt, M.C., 2020. MNRAS Advance Access. https://doi.org/10.1093/mnras/staa2385 arXiv:arXiv:2008.07406.

Lacerda, P., Jewitt, D.C., 2007. Astron. J. 133, 1393.

Lacy, J.H., Faraji, H., Sandford, S.A., Allamandola, L.J., 1998. Astrophys. J. Lett. 501, L105–L109.

Lambrechts, M., Morbidelli, A., 2016. Reconstructing the Size Distribution of the Small Body Population in the Solar System. AAS/Division for Planetary Sciences Meeting Abstracts No. 48, ID.105.08.

Langmuir, I., 1916. Phys. Ther. Rev. 8, 149.

Lesniak, M.V., Desch, S.J., 2011. Astrophys. J. 740, 118.

Levison, H.F., Duncan, M.J., 1994. Icarus 108, 18–36.

Li, J., Jewitt, D., Mutchler, M., Agarwal, J., Weaver, H., 2020. Astron. J. 159, 209.

Lisse, C.M., 2002. Earth. Moon Planets 90, 497–506.

Lisse, C.M., Bar-Nun, A., Laufer, D., Belton, M.J.S., Harris, W.M., Hsieh, H.H., Jewitt, D. C. 2013, "Cometary Ices", chapter in "The Science of Solar System Ices", Astrophys &

Space Sci Library 356, ISBN 978–1–4614-3075-9. Springer Science+Business Media New York, 455.

Lisse, C.M., et al., 2017. Astron. J. 154, 5.

Loomis, R.A., Öberg, K.I., Andrews, S.M., et al., 2020. Astrophys. J. 893, 101.

Mall, U., Altwegg, K., Balsiger, H., et al., 2016. Astrophys. J. 819, 126.

Marboeuf, U., Schmitt, B., 2014. Icarus 242, 225.

McKay, A.J., DiSanti, M.A., Kelley, M.S.P., et al., 2019. Astron. J. 158, 128.

McKinnon, W.B., Sterm, S.A., Weaver, H.A., et al., 2017. Icarus 287, 2–11.

McKinnon, W.B., Richardson, D.C., Marohnic, J.C., et al., 2020. Science 367 aay6620.

Merk, R., Prialnik, D., 2006. Icarus 183, 283–295.

Miller, G.A., Carpenter, D.K., 1964. J. Chem. Eng. Data 9, 371–373.

Moore, J.M., et al., 2018a. Icarus 300, 129–144.

Moore, J.M., Howard, A.D., Umurhan, O.M., et al., 2018b. Icarus 300, 129–144. https://doi.org/10.1016/j.icarus.2017.08.031.

Moore, J.M., et al., 2019. Scarp retreat on MU69: evidence and implications for composition and structure. In: EPSC Abstracts 13. EPSC-DPS2019-50-1.

Mousis, O., Ronnet, T., Lunine, J.I., 2019. Astrophys. J. 875, 9.

Mumma, M.J., Charnley, S., 2011. Ann. Rev. Astron Astrophys. 49, 471–524.

Nesvorný, D., Morbidelli, A., 2012. Astron. J. 144, 4.

Nesvorný, D., Youdin, A.N., Richardson, D.C., 2010. Astron. J. 140, 785–793.

Nesvorný, D., Li, R., Youdin, A.N., Simon, J.B., Grundy, W.M., 2019. Nature Astron. 3, 808–812.

Nuth, J.A., Johnson, N.M., Manning, S., 2008. Astrophys. J. Lett. 673, L225.

Öberg, K.I., Guzmán, V.V., Merchantz, C.J., et al., 2017. Astrophys. J. 839, 1.

Prialnik, D., 2002. EM&P 89, 27–52.

Prialnik, D., Bar-Nun, A., 1990. Astrophys. J. 355, 281.

Prialnik, D., Bar-Nun, A., Podolak, M., 1987. Astrophys. J. 319, 992.

Prialnik, D., Benkhoff, J., & Podolak, M. 2004, "Modeling the structure and activity of comet nuclei", chapter in Comets II, M. C. Festou, H. U. Keller, and H. A. Weaver (eds.), University of Arizona Press, Tucson, 745 pp., 359–387.

Protopapa, S., et al., 2017. Icarus 287, 218–228.

Quirico, E., Douté, S., Schmitt, B., de Bergh, C., et al., 1999. Icarus 139, 159–178.

Quirico, E., et al., 2015. EPSC Abstracts 10, EPSC2015-621.

Quirico, E., et al., 2016. Icarus 272, 32.

Reuter, D.C., Stern, S.A., Scherrer, J., et al., 2008. Space Sci. Rev. 140, 129–154.

Robbins, S.J., Beyer, R.A., Spencer, J.R., et al., 2019. JGR: Planets 124, 155–174.

Rosenberg, E.D., Prialnik, D., 2009. MNRAS Letters 399, L79.

Sandford, S.A., Allamadola, L.J., 1993a. Icarus 106, 478–488.

Sandford, S.A., Allamadola, L.J., 1993b. Astrophys. J. 417, 815–825.

Sandford, S.A., Allamandola, L.J., 1988. Icarus 76, 201–224.

Sandford, S.A., Allamandola, L.J., 1990. Icarus 87, 188–192.

Sandford, S.A., Allamadola, L.J., Geballe, T.R., 1993. Science 262, 400–402.

Schaller, E.L., Brown, M.E., 2007. Astrophys. J. 659, L61.

Schenk, P.M., Singer, K., Beyer, R., et al., 2020. Icarus 113834. https://doi.org/10.1016/j.icarus.2020.113834. https://www.sciencedirect.com/science/article/abs/pii/S0019103520302153.

Schmitt, B., Espinasse, S., Grim, R.J.A., Greenberg, J.M., Klinger, J., 1989. Physics and Mechanics of Cometary Materials (ESA SP-302; Noordwijk:ESA publications division), 65.

Schmitt, B., et al., 2017. Icarus 287, 229–260.

Schutte, W.A., Allamandola, L.J., Sandford, S.A., 1993a. Science 259, 1143–1145.

Schutte, W.A., Allamandola, L.J., Sandford, S.A., 1993b. Icarus 104, 118–137.

Sekine, Y., Genda, H., Kamata, S., Funatsu, T., 2017. Nature Astronomy 1, 0031.

Shock, E.L., McKinnon, W.B., 1993. Icarus 106, 464–477.

Singer, K., McKinnon, W.B., Gladman, B., et al., 2019. Science 363, 955–959.

Spencer, J.R., Stern, S.A., Moore, J.M., et al., 2020. Science 367 aay3999.

Steckloff, J.K., Johnson, B.C., Bowling, T., et al., 2015. Icarus 258, 430–437.

Steckloff, J.K., Lisse, C.M., Safrit, T.K., Bosh, A.S., Lyra, W. 2020, Ibid (Icarus, this issue).

Stern, S.A., 2003. Nature 424, 639–642.

Stern, S.A., et al., 2006. Nature 439, 946.

Stern, S.A., et al., 2015. Science 350, 1815.

Stern, S.A., Weaver, H.A., Spencer, J.R., et al., 2019. Science 364, 9771.

Sunshine, J.S., et al., 2006. Science 311, 1453–1455.

Tang, H., Dauphas, N., 2015. Astrophys. J. 802, 22.

Thrane, K., Bizzarro, M., Baker, J.A., 2006. Astrophys. J. 646, L159–L162.

Weaver, H.A., Buie, M.W., Buratti, B.J., et al., 2016. Science 351, 30.

Yamamoto, T., Nakagawa, N., Fukui, Y., 1983. Astron. Astrophys. 122, 171–176.

Yokochi, R., Marboeuf, U., Quirico, E., Schmitt, B., 2012. Icarus 218, 760–770.

Young, L.A., et al., 2018. Icarus 300, 174–199.